

# Feasibility of simultaneous measurement of cytosolic calcium and hydrogen peroxide in vascular smooth muscle cells

Kyung-Hwa Chang<sup>#</sup>, Jung-Min Park<sup>#</sup> & Moo-Yeol Lee<sup>\*</sup>

College of Pharmacy, Dongguk University, Goyang 410-820, Korea

**Interplay between calcium ions (Ca<sup>2+</sup>) and reactive oxygen species (ROS) delicately controls diverse pathophysiological functions of vascular smooth muscle cells (VSMCs). However, details of the Ca<sup>2+</sup> and ROS signaling network have been hindered by the absence of a method for dual measurement of Ca<sup>2+</sup> and ROS. Here, a real-time monitoring system for Ca<sup>2+</sup> and ROS was established using a genetically encoded hydrogen peroxide indicator, HyPer, and a ratiometric Ca<sup>2+</sup> indicator, fura-2. For the simultaneous detection of fura-2 and HyPer signals, 540 nm emission filter and 500 nm~ dichroic beamsplitter were combined with conventional exciters. The wide excitation spectrum of HyPer resulted in marginal cross-contamination with fura-2 signal. However, physiological Ca<sup>2+</sup> transient and hydrogen peroxide were practically measurable in HyPer-expressing, fura-2-loaded VSMCs. Indeed, distinct Ca<sup>2+</sup> and ROS signals could be successfully detected in serotonin-stimulated VSMCs. The system established in this study is applicable to studies of crosstalk between Ca<sup>2+</sup> and ROS. [BMB Reports 2013; 46(12): 600-605]**

## INTRODUCTION

Calcium ions (Ca<sup>2+</sup>) are ubiquitous intracellular secondary messengers in signaling pathways involved in the regulation of numerous cellular processes including muscular contraction, neurotransmission, secretory activity, development and differentiation (1, 2). With similar versatility, reactive oxygen species (ROS) including superoxide and hydrogen peroxide (H<sub>2</sub>O<sub>2</sub>) also play pivotal roles in various cellular functions such as proliferation, differentiation, cytoskeleton rearrangement and survival and death (3, 4). Vascular smooth muscle cells (VSMCs) are contractile cells that are of fundamental im-

portance in providing structural integrity to vessel walls. VSMCs take part in diverse physiological processes by virtue of their marked phenotypic plasticity and control over vascular tone and blood pressure by regulation of contractility. The Ca<sup>2+</sup>-mediated signaling axis is a major contraction pathway. Cytosolic Ca<sup>2+</sup> combined with calmodulin binds and activates myosin light chain kinase, which leads to myosin phosphorylation, myosin ATPase activation, and ultimately stimulates actin and myosin cross-bridge cycling (5). ROS serve as signaling molecules and modify the function of various proteins including transcription factors, kinases and phosphatases. Accordingly, ROS regulates many aspects of VSMC functions like contraction, proliferation and migration by direct and indirect effects at multiple signaling levels. Ca<sup>2+</sup> and ROS are the critical mediators in signaling pathways responsible for a variety of pathophysiological processes in VSMCs (6).

In addition to discrete signaling pathways, complicated systems of crosstalk have been reported between Ca<sup>2+</sup> and ROS in VSMCs (7, 8). Mutual interaction between Ca<sup>2+</sup> and ROS are generally ascribed to either the effect of Ca<sup>2+</sup> on ROS generation and antioxidant system, or that of ROS on the regulators and effectors of Ca<sup>2+</sup>. Indeed, ROS modify specific amino acid residues in Ca<sup>2+</sup> channels and pumps, stimulating or inhibiting these molecules, resulting in altered Ca<sup>2+</sup> distribution. Ca<sup>2+</sup> handling molecules affected by ROS include L-type voltage-gated calcium channel, Orai, transient receptor potential channel, ryanodine receptor, sarcoplasmic reticulum (SR) calcium transport ATPase (SERCA) and plasma membrane calcium-ATPase (PMCA) (2). With similar molecular mechanisms, ROS induces functional alteration of Ca<sup>2+</sup> effectors such as protein phosphatases and kinases (7, 9). On the other hand, Ca<sup>2+</sup> also influences on ROS signals by affecting multiple sources for ROS production. ROS sources affected by Ca<sup>2+</sup> include mitochondria and ROS-generating enzymes such as NADPH oxidase and xanthine oxidase (3). In general, Ca<sup>2+</sup> are required for ROS generation or their augmented production, which leads to a wide range of functional changes in VSMCs (7, 10, 11). Ca<sup>2+</sup> and ROS signals thus represent major signaling axis in VSMCs and their interplay allows for the delicate and complicate control over VSMCs physiology.

Absence of experimental methods to monitor both Ca<sup>2+</sup> and ROS has been a critical impediment to studies of the crosstalk between Ca<sup>2+</sup> and ROS signaling. Ca<sup>2+</sup> distribution can be suc-

\*Corresponding author. Tel: +82-31-961-5222; Fax: +82-31-961-5206; E-mail: mlee@dongguk.edu

<sup>#</sup>The first two authors contributed equally to this work.

<http://dx.doi.org/10.5483/BMBRep.2013.46.12.103>

Received 7 May 2013, Revised 21 May 2013, Accepted 21 May 2013

**Keywords:** Calcium, Hydrogen peroxide, HyPer, Reactive oxygen species, Vascular smooth muscle cells

cessfully visualized by fluorescence indicators such as fura-2 and fluo-4 combined with digital imaging (12). ROS, mostly superoxide or  $\text{H}_2\text{O}_2$ , can also be detected using fluorescence or luminescence probes. However, there are a few critical drawbacks in ROS probes. Most ROS indicators interact with ROS to generate fluorescence or luminescence signals, but these are irreversible redox reactions. This means that once ROS probes react with ROS, they are incapable of reflecting further decreases in ROS production. In addition, they can produce ROS upon light exposure, which results in artifactual ROS generation and signal amplification (13, 14). HyPer, a genetically encoded  $\text{H}_2\text{O}_2$  indicator, has been recently developed. HyPer is a circularly permuted yellow fluorescent protein and successfully detected temporal increase in  $\text{H}_2\text{O}_2$  upon physiological stimulation. Reaction with  $\text{H}_2\text{O}_2$  is reversible, allowing real-time measurement of  $\text{H}_2\text{O}_2$  production and elimination (15-17).

In the present study, we established methods for quantitative, real-time monitoring of  $\text{Ca}^{2+}$  and  $\text{H}_2\text{O}_2$  in live VSMCs. The ratio-metric fluorescent indicator fura-2 was used for  $\text{Ca}^{2+}$  detection and a DNA construct for HyPer was introduced into VSMCs to express cytosolic HyPer capable of detecting  $\text{H}_2\text{O}_2$  (15, 18). To observe both fura-2 and HyPer signals continuously, illumination to excite fura-2 and HyPer was provided by a high performance filter changer, and emitted light was detected with an appropriate filter and an electron multiplying charge-coupled device (EMCCD) camera. HyPer exhibited a wide range of optical dynamics between 350-550 nm, so the fluorescence signals from fura-2 and HyPer were not completely separable. However, cross-contamination of optical signals was practically allowable. Thus, both signals from physiological  $\text{Ca}^{2+}$  and  $\text{H}_2\text{O}_2$  levels could be successfully detectable distinctively. The method established in this study may well be applicable to future studies of the interplay between  $\text{Ca}^{2+}$  and  $\text{H}_2\text{O}_2$ .

## RESULTS AND DISCUSSION

### Expression of HyPer in VSMCs

Primary cultured VSMCs were difficult to transfect with plasmids using general chemical-based transfection methods that utilize lipid-based transfection reagents or calcium phosphate (19). Hence, viral transduction was employed to express HyPer in VSMCs. A gene for HyPer was subcloned into the lentiviral vector pLJM1, which was confirmed by restriction enzyme digestion. Digestion of cloned plasmids with *NheI* and *EcoRI* yielded 7.3 kb pLJM1 and 1.5 kb HyPer (Fig. 1A). Lentiviruses were generated by co-transfecting pLJM1-HyPer and packaging vectors (a mixture of pLP1, pLP2, and pVSVG plasmids) into 293FT packaging cell line. VSMCs were infected with lentivirus to express HyPer, which was confirmed by fluorescence microscopy and Western blotting. Basal fluorescence was bright enough to be observed by conventional fluorescence microscopy (Fig. 1B). Immunoblot analysis detected 52 kDa HyPer in VSMCs lysate with anti-green fluorescence protein (GFP) antibody (Fig. 1C).

### Validation of imaging system for measuring fura-2 and HyPer signals

HyPer has a wide range of excitation spectrum from below 350 to longer than 520 nm. Therefore, it is difficult to find any  $\text{Ca}^{2+}$  indicators whose excitation spectrum does not overlap with that of HyPer. With this reality, fura-2 was chosen as the  $\text{Ca}^{2+}$  indicator expected to be compatible with HyPer. Excitation wavelengths used for fura-2 (340 and 380 nm) are suitably distinct from that of HyPer. In addition, the maximal emission wavelengths were 510-520 nm for both HyPer and fura-2, which indicates that emission from both HyPer and fura-2 can be collected with an emission filter. Since the image capture rate needed to be fast enough to detect  $\text{Ca}^{2+}$  transient in VSMCs, a motorized filter rotating turret could not be used because of limited

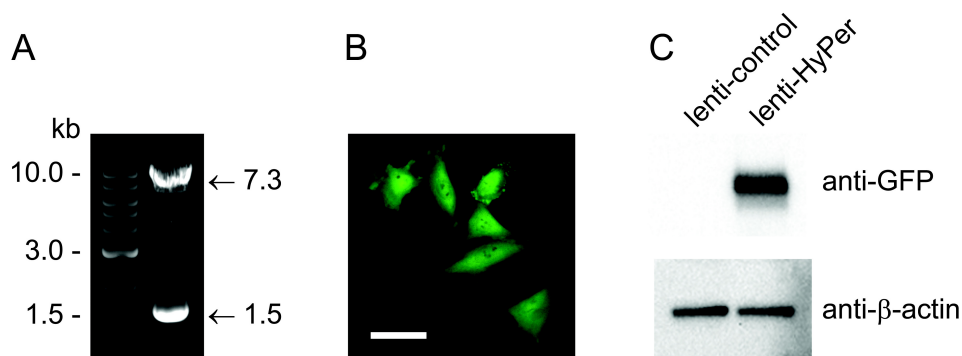


**Fig. 1.** Expression of HyPer in VSMCs. (A) Verification of cloned pLJM1-HyPer by restriction enzyme digestion. Cloned construct was digested with *NheI* and *EcoRI* and the resulting construct was resolved by agarose gel electrophoresis. Left lane: 1 kb plus DNA ladder. Right lane: 7.3 kb pLJM1 and 1.5 kb HyPer yielded from digestion. (B) Fluorescence image of HyPer-expressing VSMCs. VSMCs were infected with recombinant lentivirus carrying HyPer. The representative image was obtained 48 h post-infection. The scale bar denotes 30  $\mu\text{m}$ . (C) Western blot analysis of HyPer-expression in VSMCs. Lentivirus-infected VSMCs were lysed and subjected to SDS-PAGE and immunoblotting.

repositioning speed. Instead, an imaging system was constituted with a fixed filter set [excitation filters: 340 (320-355)/380 (375-400) nm for fura-2 and 475 (450-497) nm for HyPer, emission filter: 540 (510-570) nm, and dichroic beamsplitter: 500 nm~] in combination with conventional fluorescence microscopy. Excitation filters were installed in an external illuminator, lambda DG-4 wavelength switcher (Sutter Instruments, Novato, CA, USA) for fast and alternate illumination.

Since excitation spectra were not completely distinct from each other, a potential cross-contamination in optical signals between HyPer and fura-2 was investigated (15, 18). Emission filter and dichroic mirror were set for the detection of dual signals from both HyPer and fura-2, so they might not be as efficient as optical filters optimized for either HyPer or fura-2. To compare our filter set with conventional fura-2 or HyPer filter set, fura-2 and HyPer signals were analyzed in VSMCs. Intensities of emission signals from both 340 and 380 nm activation were diminished by approximately 35% compared with those from typical filter set for fura-2 [the same excitation filters as described above, 510 (460-557) nm emitter, and 397 nm~ dichroic mirror]. However, attenuations of each signal were quite similar in rate. Thus, the ratio of emission signals from 340 and 380 nm excitation was minimally changed. When fura-2-loaded cells were excited with 475 nm wavelength, the emission signal was only 4.6% of that obtained from 380 nm activation, indicating that HyPer signal may be affected by fura-2, but such influence was practically negligible. In the subsequent experiments, HyPer was examined under our imaging system. Compared with conventional filter set for GFP [the same excitation filter as described above, 530 (505-562) nm emitter, and 490 nm~ dichroic mirror], emission was increased by 8.4%. When HyPer was excited with 340 and 380 nm, intensities of emission were approximately 4.0% and 28.8% of those from 475 nm excitation. Emission from excited HyPer at 340 nm appeared not to be critical, but emission signals from 380 nm excitation was not negligible. Taken together,

er, the results indicated that the HyPer signal is minimally affected by the presence of fura-2. However, fura-2 signals, especially emission from 380 nm activation, may be influenced by HyPer. Thus, fura-2 signals must be interpreted with caution when fura-2 and HyPer were examined simultaneously.

To test the feasibility of measuring  $\text{Ca}^{2+}$  and  $\text{H}_2\text{O}_2$ , fura-2 or HyPer signal was analyzed in fura-2-loaded VSMCs or VSMCs expressing HyPer. Cytosolic  $\text{Ca}^{2+}$  increase was evoked by the application of 75 mM  $\text{K}^+$ , which elicits membrane depolarization and induces  $\text{Ca}^{2+}$  influx through opening L-type voltage-gated  $\text{Ca}^{2+}$  channels (1, 2). As expected, mild but apparent  $\text{Ca}^{2+}$  increase was detected without significant change in signal from 475 nm excitation (Fig. 2, left panel). When 10  $\mu\text{M}$   $\text{H}_2\text{O}_2$  was used to treat HyPer-expressing cells, HyPer signal from 475 nm activation was observed without change in the ratio of emission signals from 340 and 380 nm activation (Fig. 2, right panel). These results indicated that physiological increments of  $\text{Ca}^{2+}$  and  $\text{H}_2\text{O}_2$  can be detected under our experimental system without optical artifact caused by cross-contamination. For further validation, a similar experiment was performed with HyPer-expressing, fura-2-loaded VSMCs (Fig. 3A). When these cells were treated with 75 mM  $\text{K}^+$ ,  $\text{Ca}^{2+}$  increase was detected in the absence of apparent alteration of HyPer signal (Fig. 3B, left panels). Treatment of cells with 10  $\mu\text{M}$   $\text{H}_2\text{O}_2$  elicited the increase in HyPer signals without significant alteration of fura-2 signal (Fig. 3B, middle panels). To examine simultaneous measurement of HyPer and fura-2 signals, both 75 mM  $\text{K}^+$  and 10  $\mu\text{M}$   $\text{H}_2\text{O}_2$  were applied to these cells. As shown in the right panels of Fig. 3, both  $\text{Ca}^{2+}$  and  $\text{H}_2\text{O}_2$  increases were observed in the same regions of cells. Increases in  $\text{Ca}^{2+}$  and  $\text{H}_2\text{O}_2$  were exaggerated by concomitant treatment with 75 mM  $\text{K}^+$  and 10  $\mu\text{M}$   $\text{H}_2\text{O}_2$  compared with those elicited by either 75 mM  $\text{K}^+$  and 10  $\mu\text{M}$   $\text{H}_2\text{O}_2$  (Fig. 3B). These results indicated the presence of mutual interaction between  $\text{Ca}^{2+}$  and  $\text{H}_2\text{O}_2$  in VSMCs. Why the combined treatment of high concentration of  $\text{K}^+$  and  $\text{H}_2\text{O}_2$  enhanced each

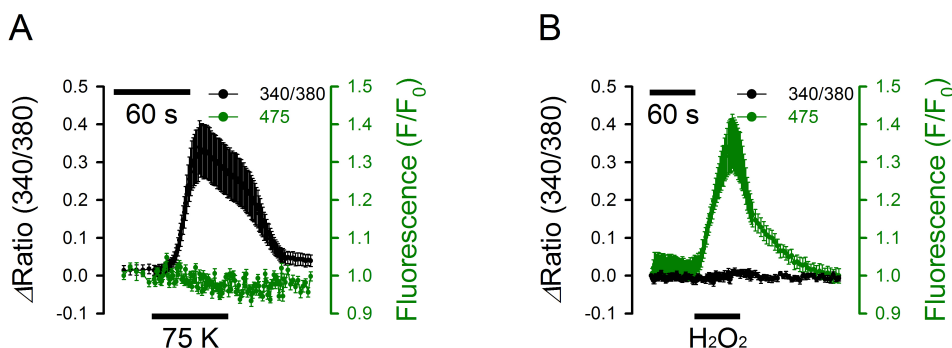


**Fig. 2.** Validation of optical property. (A) Fura-2-loaded VSMCs were stimulated with 75 mM  $\text{K}^+$ . (B) VSMCs expressing HyPer were treated with 10  $\mu\text{M}$   $\text{H}_2\text{O}_2$ . Images were obtained with the filter set designed for simultaneous detection of fura-2 and HyPer. Time courses of signal from fura-2 or HyPer was traced with black or green line, respectively. Bars at the bottom of each panel indicate the periods of 75 mM  $\text{K}^+$  or 10  $\mu\text{M}$   $\text{H}_2\text{O}_2$  application. Values are mean  $\pm$  standard error.  $n = 14$  or 19 for black or green lines in (A) and  $n = 7$  in (B).

signaling remains unclear and requires more study. Taken together, it is feasible to monitor cytosolic Ca<sup>2+</sup> and H<sub>2</sub>O<sub>2</sub> signals with fura-2 and HyPer independently and simultaneously in live cells under our experimental system.

### Simultaneous detection of Ca<sup>2+</sup> and H<sub>2</sub>O<sub>2</sub> signals elicited by 5-HT

With established imaging system, response of VSMCs to serotonin (5-hydroxytryptamine, 5-HT) was examined. Ca<sup>2+</sup> transient by 5-HT has long been described in VSMCs (20). In addition, 5-HT generates ROS as downstream signaling molecules mediating mitogenesis in VSMCs although their origins and effectors have not been fully elucidated (21, 22). VSMCs expressing HyPer were loaded with fura-2 (Fig. 4A), and Ca<sup>2+</sup> and H<sub>2</sub>O<sub>2</sub> signals were continuously recorded during

experiment. Treatment of 10 μM 5-HT evoked a prompt Ca<sup>2+</sup> transient and subsequent H<sub>2</sub>O<sub>2</sub> generation (Fig. 4B). The blue, red and purple tracings in Fig. 4B represent fura-2 signals from the boxed areas shown in Fig. 4A. The green tracings indicate HyPer signals in the corresponding regions.

Ca<sup>2+</sup> transient and H<sub>2</sub>O<sub>2</sub> production have never been detected simultaneously in live cells. From the present study, it is now clear that Ca<sup>2+</sup> transient precedes ROS production and H<sub>2</sub>O<sub>2</sub> production is followed by Ca<sup>2+</sup> transient in 5-HT-stimulated cells. It is unclear whether Ca<sup>2+</sup> affects H<sub>2</sub>O<sub>2</sub> signal and vice versa. With established methods in this study, possible interactions between ROS and Ca<sup>2+</sup> signaling will be addressed through further study.

In conclusion, fura-2 and HyPer can be a particularly useful combination for simultaneous measurement of Ca<sup>2+</sup> and ROS

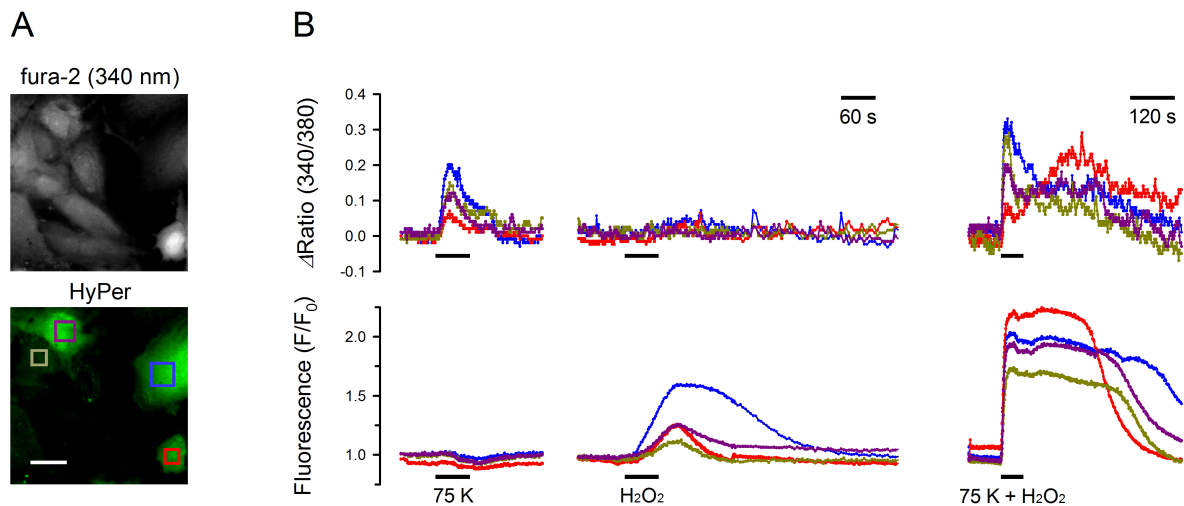


**Fig. 3.** Simultaneous measurement of fura-2 and HyPer signals. HyPer-expressing, fura-2-loaded VSMCs were treated with 75 mM K<sup>+</sup> and/or 10 μM H<sub>2</sub>O<sub>2</sub>. Intracellular Ca<sup>2+</sup> and H<sub>2</sub>O<sub>2</sub> were continuously detected under imaging system. (A) Cellular images obtained from fura-2 (activated at 340 nm wavelength) or HyPer signals. (B) Tracings of fura-2 and HyPer signals. Ca<sup>2+</sup> and H<sub>2</sub>O<sub>2</sub> signals detected by fura-2 or HyPer were shown in upper and lower panels, respectively. Each line colored by red, blue, purple, or dark yellow represents the signals obtained from regions boxed with the corresponding colors in (A). Bars at the bottom of each tracing indicate the application of 75 mM K<sup>+</sup> and/or 10 μM H<sub>2</sub>O<sub>2</sub>.

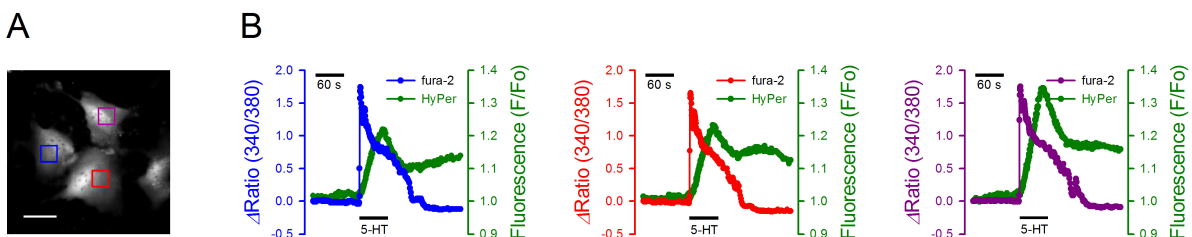


**Fig. 4.** Ca<sup>2+</sup> and H<sub>2</sub>O<sub>2</sub> signals in VSMCs stimulated by 5-HT. (A) Images of HyPer-expressing VSMCs. (B) Ca<sup>2+</sup> and H<sub>2</sub>O<sub>2</sub> signals detected by fura-2 and HyPer. Each line colored by red, blue, or purple represents the Ca<sup>2+</sup> signals obtained from the regions boxed with the corresponding colors in (A). H<sub>2</sub>O<sub>2</sub> signals in each box were presented with green lines together with the Ca<sup>2+</sup> signal in the same regions. Bars at the bottom of each tracing indicate the application of 1 μM 5-HT. The scale bar denotes 20 μm.

in live cells. Dual real-time monitoring system established in this study will be a powerful method for future understanding of the signal transduction network of Ca<sup>2+</sup> and ROS in VSMCs.

## MATERIALS AND METHODS

### Reagents

HyPer-cyto plasmid was purchased from Evrogen (Moscow, Russia). Anti-GFP and horseradish peroxidase-conjugated anti-rabbit IgG antibodies were obtained from Cell Signaling Technology (Beverly, MA, USA). T4 DNA ligase, Tag DNA polymerase, restriction enzymes NheI and EcoRI were purchased from Takara Bio (Otsu, Japan). Other chemicals and sources were as follows: pLJM1-GFP lentiviral vector (Addgene, Cambridge, MA, USA); pGEM-T vector (Promega, Madison, WI, USA); H<sub>2</sub>O<sub>2</sub> (Samchun Chemical, Pyeongtaek, Korea); 5-HT (Sigma-Aldrich, St. Louis, MO, USA); fura-2/AM (Invitrogen, Carlsbad, CA, USA). All other chemicals used were of the highest purity available and purchased from standard suppliers.

### Animals

All animal experiments were conducted in accordance with protocols approved by the Ethics Committee of Animal Service Center at Dongguk University. Male Sprague-Dawley rats (5-6 weeks of age) were purchased from Daehan Biolink (Eumseong, Korea), and acclimated for 1 week before experiments. The laboratory animal facility was maintained at a constant temperature and humidity with a 12 h light/dark cycle. Food and water were provided *ad libitum*.

### Cells and cell culture

VSMCs were isolated from rat thoracic aorta by enzymatic digestion as described previously (23). Briefly, the aortas were excised, cut open longitudinally and cleaned of connective tissue, fat and endothelium. Following digestion with collagenase and elastase, individual cells were plated on coverslips in a 24 well plate, and grown in Dulbecco's modified Eagle's medium (DMEM) supplemented with 10% fetal bovine serum, 100 U/ml penicillin and 100 µg/ml streptomycin. The 293FT embryonal human kidney cell line was purchased from Invitrogen. Cells were cultured in DMEM containing 10% calf serum, 2 mM L-glutamine, 100 U/ml penicillin and 0.1 mg/ml streptomycin. Both VSMCs and 293FT cells were maintained at 37°C and 5% CO<sub>2</sub> in a humidified incubator, and were subcultured when they reached 80-90% confluence.

### Construction of HyPer expression plasmids

HyPer cDNA was amplified by polymerase chain reaction (PCR) from pHyPer-cyto plasmid. The sense primer was 5'-GCTAGCCGCCACCATGGAGATGGCAAGCC-3' and the anti-sense sequence was 5'-GAATTCTTAAACCGCCTGTTTTAA AAC-3'. The amplified HyPer fragments were inserted into the pGEM-T vector to yield pGEM-T-HyPer, which was confirmed by direct DNA sequencing. The pGEM-T-HyPer plasmid was

double digested with NheI and EcoRI, and the resulting product was inserted into NheI-EcoRI sites in the lentiviral vector pLJM1-GFP to generate pLJM1-HyPer. This plasmid was transformed into *Escherichia coli* XL1-Blue.

### Recombinant lentivirus construction, transduction and the expression of HyPer

To produce recombinant lentiviruses encoding HyPer, 293FT cells were transfected with pLJM1-HyPer plasmid and ViraPower Lentiviral Packaging Mix (Invitrogen) using Lipofectamine 2000 (Invitrogen). The virus-containing supernatant was collected 48 h after transfection and filtered with a 0.45 µm membrane filter. Virus titers were determined according to manufacturer's instruction for Lenti-X qRT-PCR titration kit. For viral infection, VSMCs were seeded at a density of 1 × 10<sup>5</sup> cells in a 60 mm plate and infected with lentivirus in the presence of 8 µg/ml polybrene. Cells were lysed with RIPA buffer after 48 h and protein content was quantified with a bicinchoninic acid (BCA) protein assay kit. Equal aliquots of protein samples were resolved by sodium dodecyl sulfate-polyacrylamide gel electrophoresis. Developed proteins on gel were transferred to a polyvinylidene difluoride membrane. HyPer was probed with anti-GFP antibody and a horseradish peroxidase-conjugated anti-rabbit IgG antibody. Following the application of Immobilon Western detection reagents (Millipore, Billerica, MA), chemiluminescence images were obtained and analyzed with Molecular Imager ChemiDoc XRS+ imaging systems (Bio-Rad Laboratories, Hercules, CA, USA).

### Measurement of Ca<sup>2+</sup> and H<sub>2</sub>O<sub>2</sub> in live cells

Intracellular Ca<sup>2+</sup> level and H<sub>2</sub>O<sub>2</sub> were measured by digital imaging using fura-2 and HyPer, respectively, referring to previously described methods (23). VSMCs expressing HyPer were grown on coverslips for 24-48 h and were loaded with fura-2 by incubation for 60 min in physiological salt solution (PSS; 140 mM NaCl, 5 mM KCl, 5 mM NaHCO<sub>3</sub>, 1.8 mM CaCl<sub>2</sub>, 1.4 mM MgCl<sub>2</sub>, 1.2 mM NaH<sub>2</sub>PO<sub>4</sub>, 11.5 mM glucose and 10 mM HEPES, pH 7.4) containing 1 µM fura-2/AM and 1% bovine serum albumin. Coverslips were mounted in a perfusion chamber on the microscope stage and were superfused with PSS at a rate of 2 ml/min. All experiments were performed at 33°C. Cells were imaged with an Eclipse Ti-U inverted microscope equipped with a S Fluor 40X (N.A. 1.30, oil) objective lens (Nikon, Tokyo, Japan) and an Evolve 512 EMCCD camera (Photometrics, Tucson, AZ, USA). Illumination was provided by a model DG-4 filter changer (Sutter Instruments). Filter sets (Semrock, Rochester, NY, USA) used were: excitation=475 (450-497) nm and emission=530 (505-562) nm for HyPer, and excitation=340 (320-355) nm/380 (375-400) nm and emission=510 (460-557) nm for fura-2. For simultaneous measurement of HyPer and fura-2, exciter with 540 (510-570) nm excitation wavelength was used in combination with the three different emission wavelengths for HyPer and fura-2 as described above. Images were ac-

quired and analyzed with a Meta Imaging System (Molecular Devices, Sunnyvale, CA, USA).

### Acknowledgements

This work was supported by the GRRC program of Gyeonggi province (GRRC-DONGGUK2012-B01, Development of new health supplements/therapeutics for neurodegenerative diseases) and the Bio & Medical Technology Development Program of the National Research Foundation (NRF) funded by the Korean government (MEST) (No. 2012053532).

### REFERENCES

1. Berridge, M. J., Bootman, M. D. and Roderick, H. L. (2003) Calcium signalling: dynamics, homeostasis and remodelling. *Nat. Rev. Mol. Cell. Biol.* **4**, 517-529.
2. Berridge, M. J. (2008) Smooth muscle cell calcium activation mechanisms. *J. Physiol.* **586**, 5047-5061.
3. Lee, M. Y. and Griendling, K. K. (2008) Redox signaling, vascular function, and hypertension. *Antioxid. Redox Signal.* **10**, 1045-1059.
4. Ray, P. D., Huang, B. W. and Tsuji, Y. (2012) Reactive oxygen species (ROS) homeostasis and redox regulation in cellular signaling. *Cell Signal.* **24**, 981-990.
5. Marchand, A., Abi-Gerges, A., Saliba, Y., Merlet, E. and Lompre, A. M. (2012) Calcium signaling in vascular smooth muscle cells: from physiology to pathology. *Adv. Exp. Med. Biol.* **740**, 795-810.
6. Park, J. G. and Oh, G. T. (2011) The role of peroxidases in the pathogenesis of atherosclerosis. *BMB Rep.* **44**, 474-505.
7. Trebak, M., Ginnan, R., Singer, H. A. and Jourdain, D. (2010) Interplay between calcium and reactive oxygen/nitrogen species: an essential paradigm for vascular smooth muscle signaling. *Antioxid. Redox Signal.* **12**, 657-674.
8. Yan, Y., Wei, C. L., Zhang, W. R., Cheng, H. P. and Liu, J. (2006) Cross-talk between calcium and reactive oxygen species signaling. *Acta Pharmacol. Sin.* **27**, 821-826.
9. Shimoda, L. A. and Undem, C. (2010) Interactions between calcium and reactive oxygen species in pulmonary arterial smooth muscle responses to hypoxia. *Respir. Physiol. Neurobiol.* **174**, 221-229.
10. Gordeeva, A. V., Zvyagilskaya, R. A. and Labas, Y. A. (2003) Cross-talk between reactive oxygen species and calcium in living cells. *Biochemistry (Mosc)* **68**, 1077-1080.
11. Rosado, J. A., Redondo, P. C., Salido, G. M. and Pariente, J. A. (2006) Calcium signalling and reactive oxygen species in non-excitable cells. *Mini. Rev. Med. Chem.* **6**, 409-415.
12. Paredes, R. M., Etzler, J. C., Watts, L. T., Zheng, W. and Lechleiter, J. D. (2008) Chemical calcium indicators. *Methods* **46**, 143-151.
13. Choi, W. G., Swanson, S. J. and Gilroy, S. (2012) High-resolution imaging of Ca<sup>2+</sup>, redox status, ROS and pH using GFP biosensors. *Plant J.* **70**, 118-128.
14. Marchesi, E., Rota, C., Fann, Y. C., Chignell, C. F. and Mason, R. P. (1999) Photoreduction of the fluorescent dye 2'-7'-dichlorofluorescein: a spin trapping and direct electron spin resonance study with implications for oxidative stress measurements. *Free Radic. Biol. Med.* **26**, 148-161.
15. Belousov, V. V., Fradkov, A. F., Lukyanov, K. A., Staroverov, D. B., Shakhbazov, K. S., Terskikh, A. V. and Lukyanov, S. (2006) Genetically encoded fluorescent indicator for intracellular hydrogen peroxide. *Nat. Methods* **3**, 281-286.
16. Bilan, D. S., Pase, L., Joosen, L., Gorokhovatsky, A. Y., Ermakova, Y. G., Gadella, T. W., Grabher, C., Schultz, C., Lukyanov, S. and Belousov, V. V. (2013) HyPer-3: A Genetically Encoded H<sub>2</sub>O<sub>2</sub> Probe with Improved Performance for Ratiometric and Fluorescence Lifetime Imaging. *ACS Chem. Biol.* **8**, 535-542.
17. Markvicheva, K. N., Bilan, D. S., Mishina, N. M., Gorokhovatsky, A. Y., Vinokurov, L. M., Lukyanov, S. and Belousov, V. V. (2011) A genetically encoded sensor for H<sub>2</sub>O<sub>2</sub> with expanded dynamic range. *Bioorg. Med. Chem.* **19**, 1079-1084.
18. Grynkiewicz, G., Poenie, M. and Tsien, R. Y. (1985) A new generation of Ca<sup>2+</sup> indicators with greatly improved fluorescence properties. *J. Biol. Chem.* **260**, 3440-3450.
19. Elmadbouh, I., Rossignol, P., Meilhac, O., Vranckx, R., Pichon, C., Pouzet, B., Midoux, P. and Michel, J. B. (2004) Optimization of in vitro vascular cell transfection with non-viral vectors for in vivo applications. *J. Gene. Med.* **6**, 1112-1124.
20. Van Nueten, J. M., Janssens, W. J. and Vanhoutte, P. M. (1985) Serotonin and vascular reactivity. *Pharmacol. Res. Commun.* **17**, 585-608.
21. Lee, S. L., Wang, W. W., Finlay, G. A. and Fanburg, B. L. (1999) Serotonin stimulates mitogen-activated protein kinase activity through the formation of superoxide anion. *Am. J. Physiol.* **277**, L282-291.
22. Lee, S. L., Wang, W. W. and Fanburg, B. L. (1998) Superoxide as an intermediate signal for serotonin-induced mitogenesis. *Free Radic. Biol. Med.* **24**, 855-858.
23. Lee, M. Y., Song, H., Nakai, J., Ohkura, M., Kotlikoff, M. I., Kinsey, S. P., Golovina, V. A. and Blaustein, M. P. (2006) Local subplasma membrane Ca<sup>2+</sup> signals detected by a tethered Ca<sup>2+</sup> sensor. *Proc. Natl. Acad. Sci. U. S. A.* **103**, 13232-13237.